On the Impact of ^{16}O Scattering on Integral Benchmarks

Andrej Trkov

International Atomic Energy Agency, Vienna, Austria

December 2014

Background

The Working Party on Evaluation Cooperation of the OECD set up a subgroup WPEC-SG40 (alias CIELO) to focus on the evaluated nuclear data of the major nuclides in reactor technology, namely ^{1}H, ^{16}O, ^{56}Fe, ^{235}U, ^{238}U and ^{239}Pu. Different research groups in various parts of the world are working on improved evaluated nuclear data and their uncertainties for these nuclides; the ultimate test of improvement is the performance of the data in simulating integral experiments.

Two evaluations for ^{16}O have been offered to CIELO for testing: one by L. Leal from the Oak Ridge National Laboratory (labelled "ornl4"), based on SAMMY resonance analysis with resonance parameters inserted into the ENDF/B-VII.1 evaluation, and the other by G. Hale from the Los Alamos National Laboratory, which extends to 6.3 MeV. The Hale evaluation requires some additional manipulation to make a complete ENDF file that can be used in benchmark analysis.

The objective of the present work is to investigate the impact that these new evaluations have on integral benchmarks from the ICSBEP compilation and to search for cancellation effects in the biases introduced by different evaluations of other materials.

File description

The ENDF file by Leal is complete and can be processed with NJOY2012. Two ACE libraries were prepared: one (labelled "o16lealxs" with the cross sections reconstructed from the resonance parameters while the angular distributions remained as in the original file (based on ENDF/B-VII.1 data), and the second (labelled "o16lealad") in which the angular distributions were reconstructed from the resonance parameters.

The ENDF file by Hale required additional processing. First, the original file was processed with LINEAR. The cross sections were extracted and inserted into the ENDF/B-VII.1 evaluation in the available energy range to produce the file labelled "o16halexs". Secondly, the original angular distributions were inserted into the "o16halexs" file in the available energy range to produce the file labelled "o16halead". Both files were processed to make the corresponding ACE files.

At the NEMEA-7 Conference C. Lubitz drew attention to a possible problem in the ^{16}O thermal scattering cross section reported by Roubtsov at the PHYSOR-2012 conference, arguing that the zero-Kelvin scattering cross section at thermal energy of 3.852 barns in the ENDF/B-VII.1 library is too high by 3.5 %. The values in the new files, evaluated as 3.784 barns by Leal and 3.804 barns by

Hale are lower, but not as low as suggested by Lubitz. The evaluators' decisions require some clarification.

The differences in the elastic cross sections evaluated by Leal and Hale at higher energies are shown in Figures 1 and 2. In the 100 keV energy region the Leal evaluation is lower by up to 4 %. The differences at higher energies increase. There seems to be some shift in the position of the low-cross section window in the elastic cross section near 2.3 MeV.

The capture cross section in the Hale evaluation is higher and seems to have some background contribution between the resonances, but the differences in the capture cross section are probably less important due to the low value of the cross sections.

The alpha-emission cross sections in the Hale evaluation are significantly higher, as seen from Figure 4, particularly in some of the narrow resonances, but even in the plateau between the resonances they differ by as much as 50 %, as shown in Figure 5. Using the new trial feature on the IAEA EXFOR interface the inverse reaction $^{13}N(\alpha,n)^{16}O$ can be displayed. Figure 5a clearly shows that Hale followed the Bair data, while Leal followed closely the Harisopulos data, although above 4 MeV some differences can be observed, as shown in Figure 5b. The differences need to be resolved before the final evaluation is assembled.

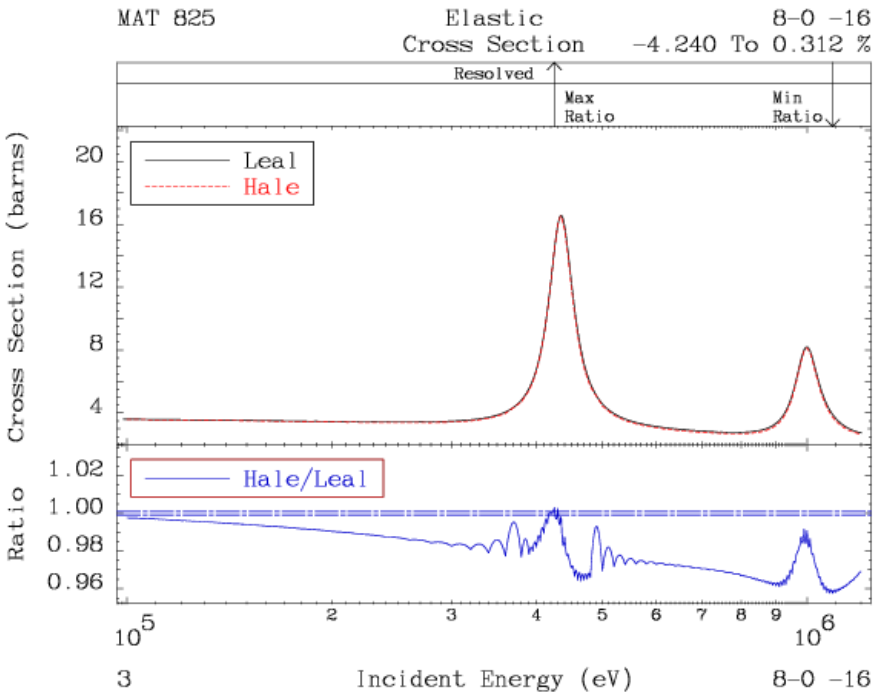

Figure 1: Comparison of the ^{16}O elastic scattering cross sections between the Leal and the Hale evaluation in the 100 keV energy region.

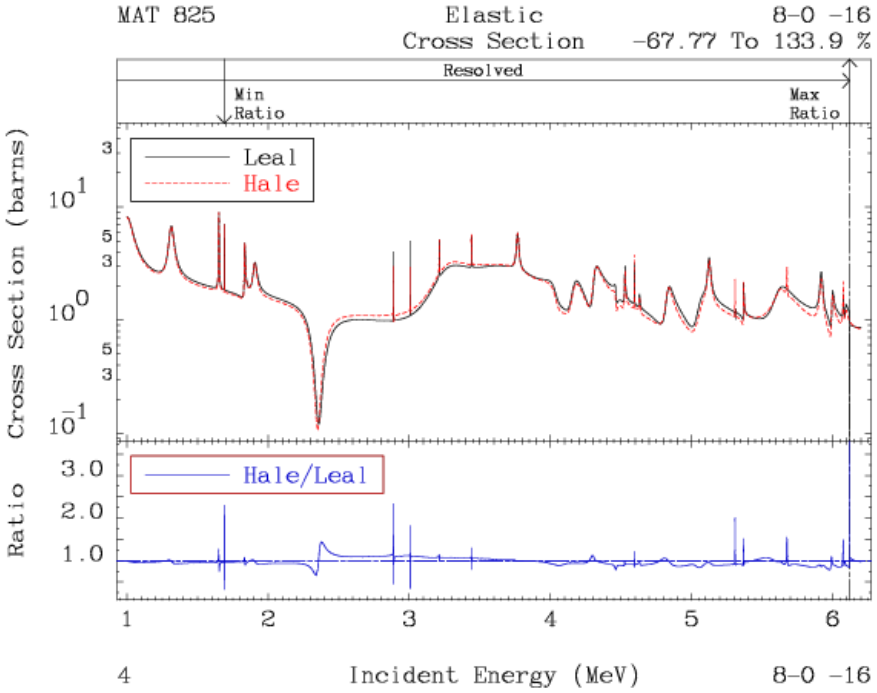

Figure 2: Comparison of the ^{16}O elastic scattering cross sections between the Leal and the Hale evaluation in the MeV energy region.

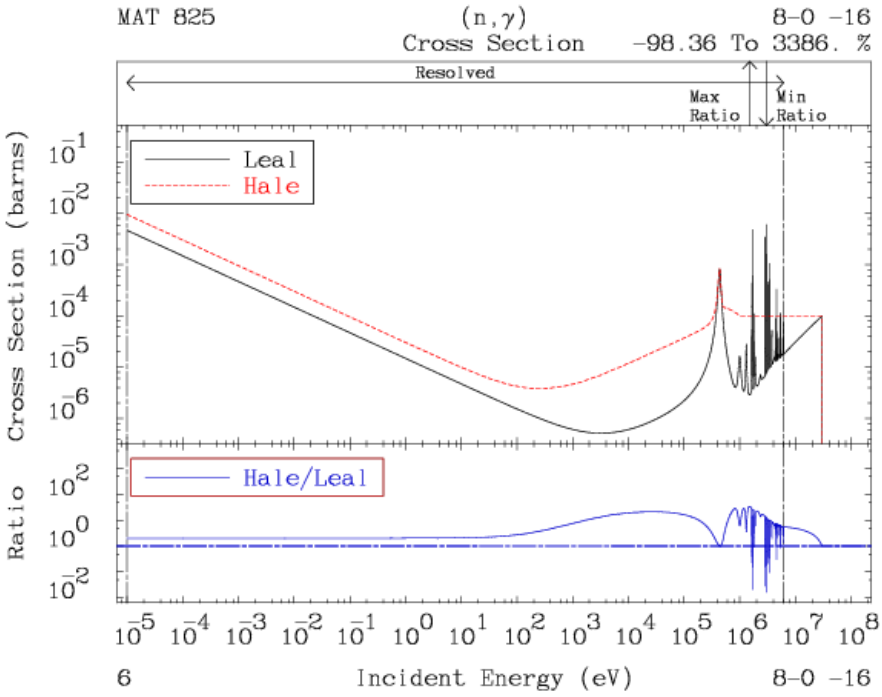

Figure 3: Comprison of the ^{16}O capture cross sections between the Leal and the Hale evaluation.

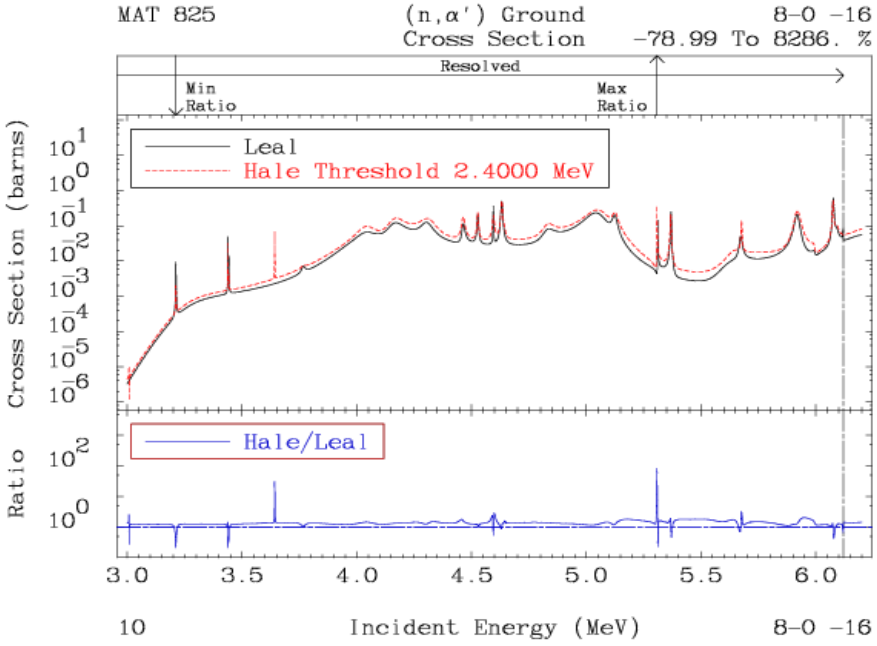

Figure 4: Comprison of the ^{16}O alpha-emission cross sections between the Leal and the Hale evaluation.

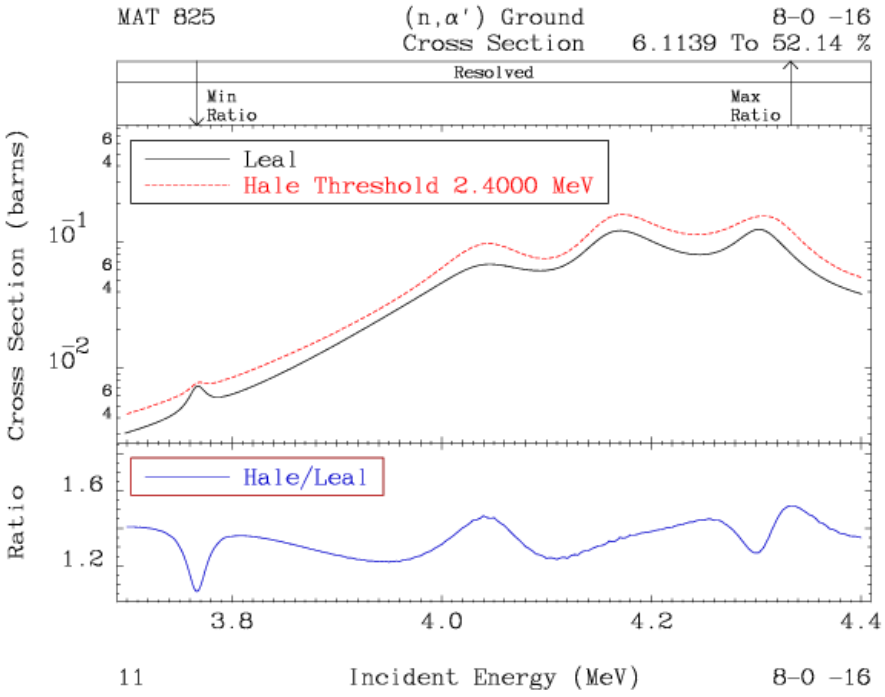

Figure 5: Comparison of the ^{16}O alpha-emission cross sections between the Leal and the Hale evaluation.

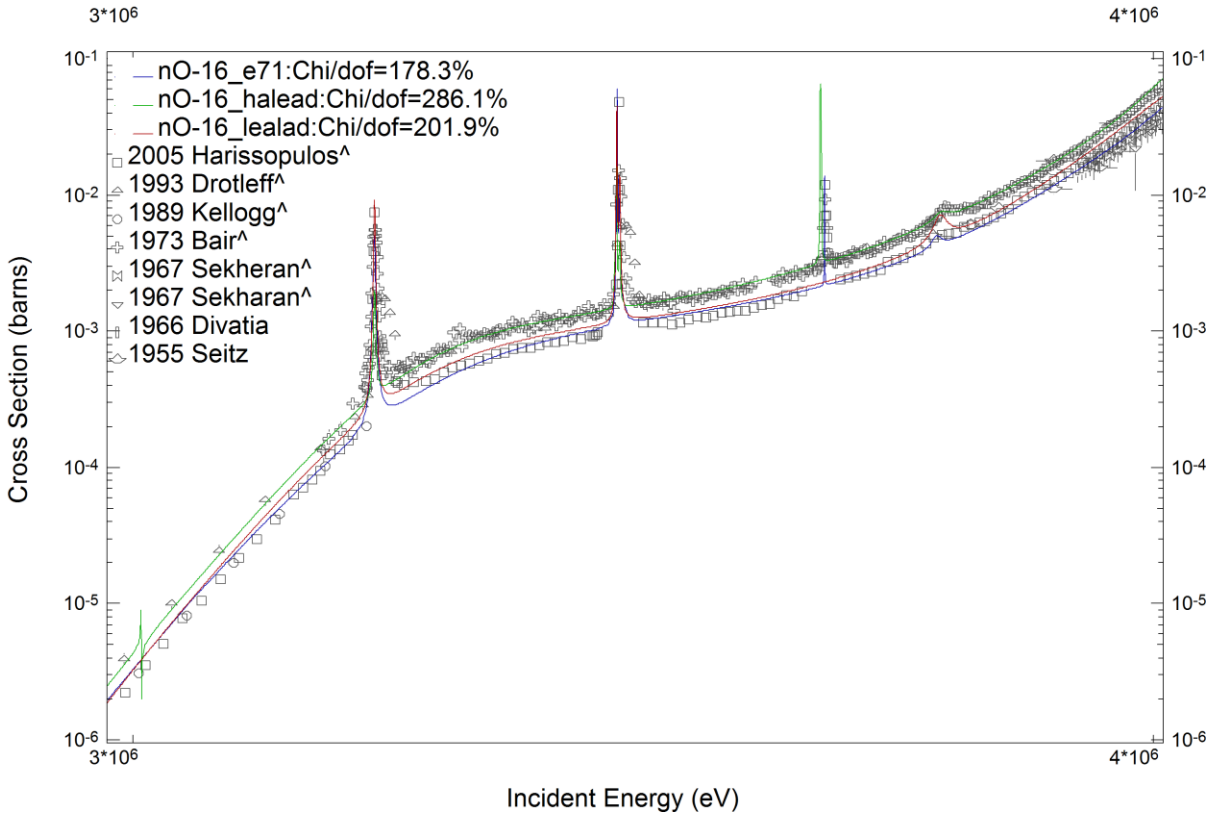

Figure 5a:

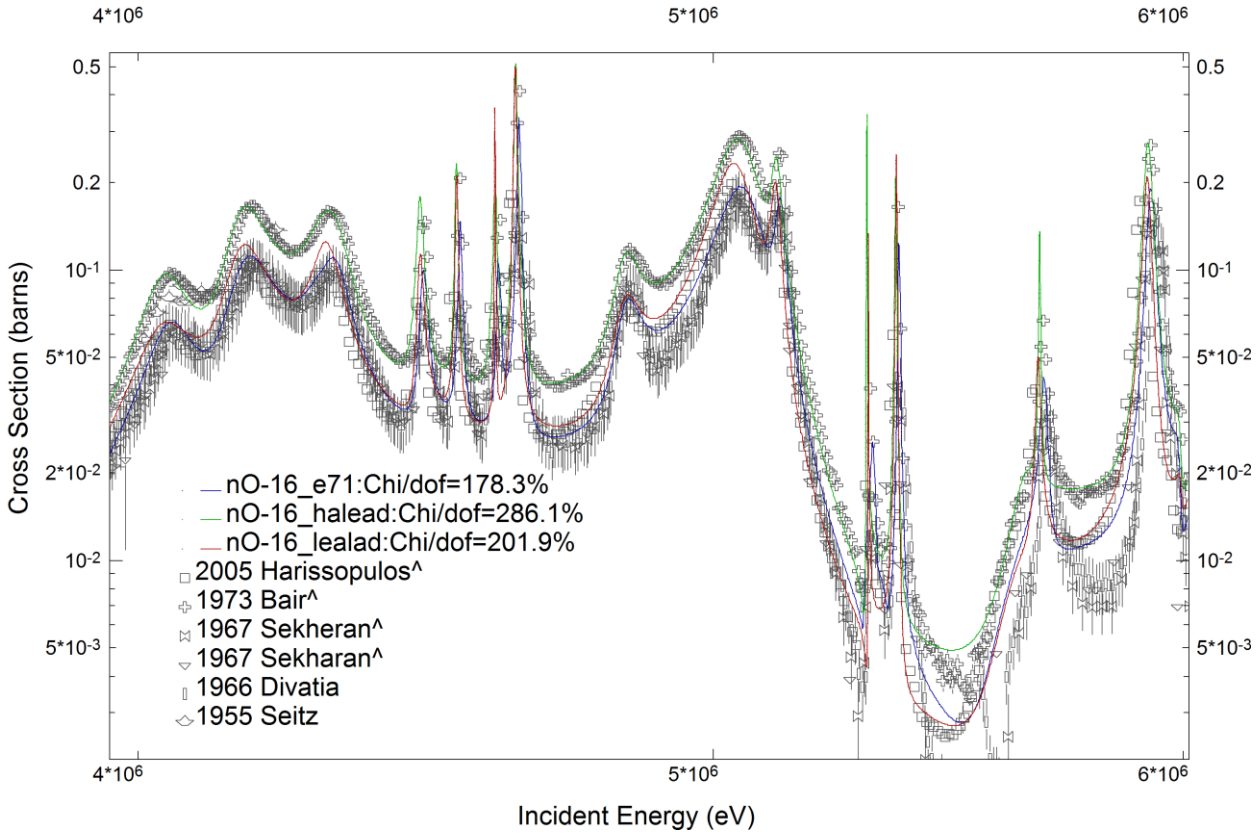

Figure 5b:

The average cosine of elastic scattering is a quantity that allows a first-order comparison between angular distributions. A comparison of the evaluations with experimental data is shown in Figure 6. There seem to be a significant discrepancy between the data sets around 2 MeV, which is the region of the low cross section window. An expanded plot emphasizing the data by Lister is shown in Figure 7. Near 3 MeV the ENDF/B-VII.1 and Leal evaluations lie close to the low-energy data points by Lister. The Hale evaluation is closer to the data by Drigo. Between 3 MeV and 4 MeV all evaluations lie slightly above the data of Lister. This information is complementary to the experimental information used by the evaluators, which may be more complete and reliable.

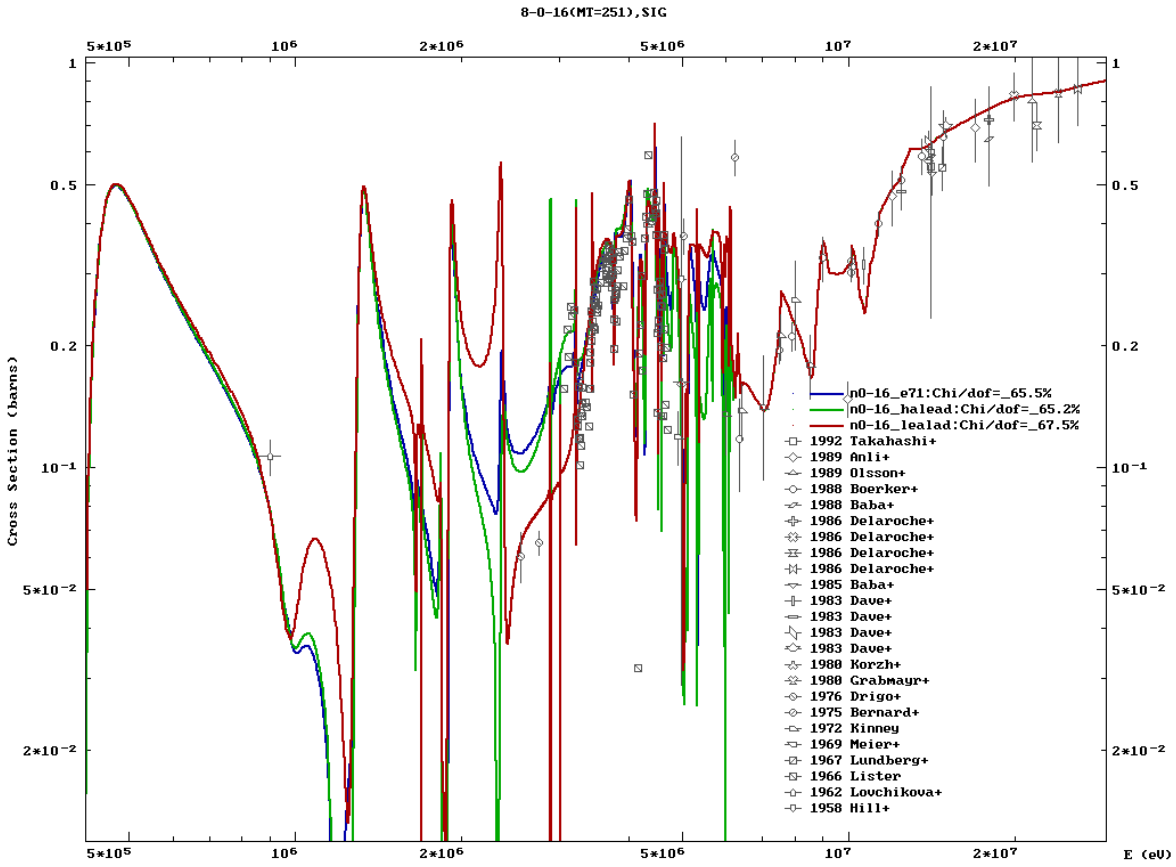

Figure 6: Comparison of mu-bar from different evaluations and experimental data.

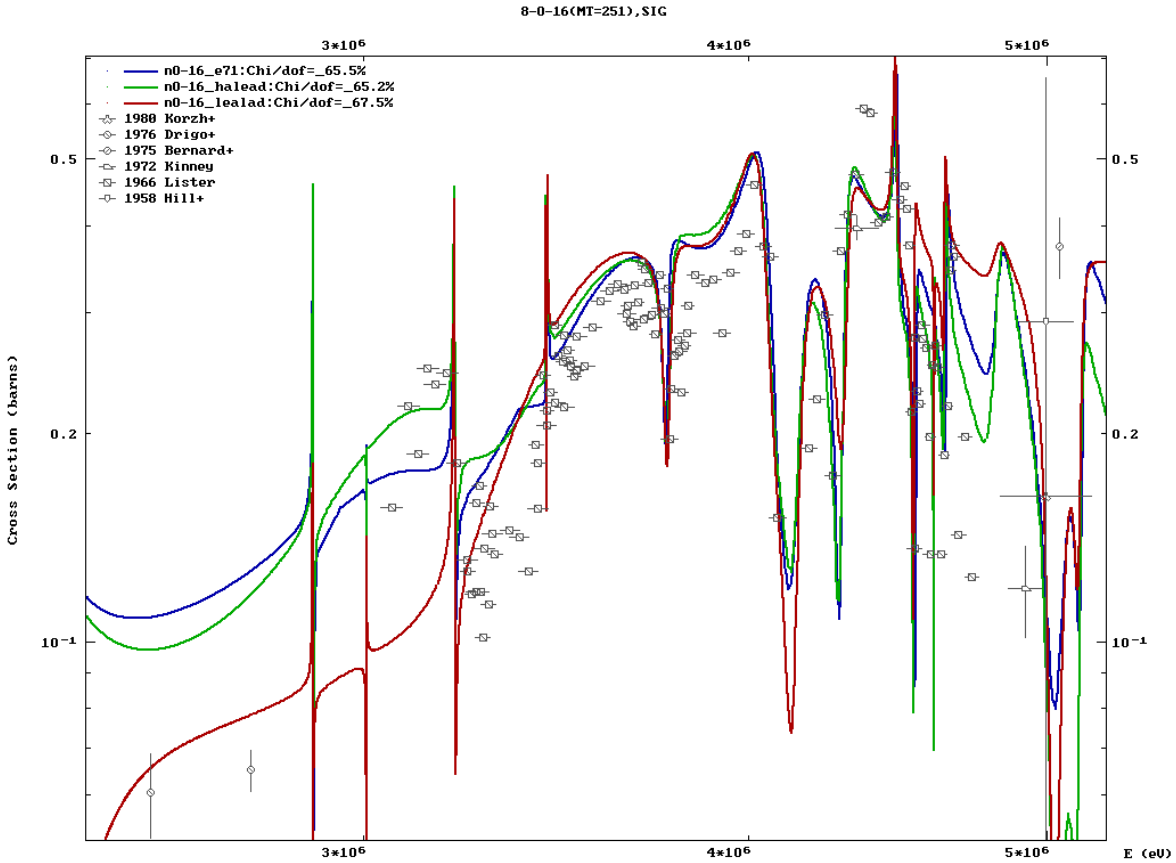

Figure 7: Expanded plot of mu-bar from different evaluations in comparison with experimental data.

Benchmark Results

The impact of the two 16O evaluations on ICSBEP benchmarks in comparison with pure ENDF/B-VII.1 data was investigated. The following files in ACE format were prepared:

o16e71	Pure ENDF/B-VII.1 evaluation.
o16lealxs	Cross sections in the ENDF/B-VII.1 file replaced by those reconstructed from the resonance parameters of Leal.
o16lealad	Cross sections AND elastic scattering angular distributions in the ENDF/B-VII.1 file replaced by those reconstructed from the resonance parameters of Leal.
o16halexs	Cross sections in the ENDF/B-VII.1 file replaced by those from the Hale evaluation.
o16halead	Cross sections AND elastic scattering angular distributions in the ENDF/B-VII.1 file replaced by those from the Hale evaluation.
O16haleadx	File “o16halead” with elastic scattering cross section below 40 keV reduced to 3.722 barns.

Table 1: List of benchmarks considered in the analysis

ICSBEP name	Short name	Common name
HEU-COMP-INTER-003	hci003-1	COMET-UH3-1
HEU-COMP-INTER-003	hci003-4	COMET-UH3-4
HEU-COMP-INTER-003	hci003-6	COMET-UH3-6
HEU-COMP-INTER-003	hci003-7	COMET-UH3-7
HEU-COMP-MIXED-003	hcm003-1	hcm003-1
HEU-COMP-THERM-007	hct007-1	hct007-1
HEU-COMP-THERM-007	hct007-2	hct007-2
HEU-COMP-THERM-015	hct015-11	SB-1
HEU-COMP-THERM-015	hct015-15	SB-5
HEU-COMP-THERM-021	hct021-01	TUPE-001
HEU-COMP-THERM-021	hct021-02	TUPE-002
HEU-COMP-THERM-021	hct021-03	TUPE-003
HEU-COMP-THERM-021	hct021-04	TUPE-004
HEU-COMP-THERM-021	hct021-05	TUPE-005
HEU-COMP-THERM-021	hct021-06	TUPE-006
HEU-COMP-THERM-021	hct021-07	TUPE-007
HEU-COMP-THERM-021	hct021-08	TUPE-008
HEU-COMP-THERM-021	hct021-09	TUPE-009
HEU-COMP-THERM-021	hct021-10	TUPE-010
HEU-COMP-THERM-021	hct021-11	TUPE-011
HEU-COMP-THERM-021	hct021-12	TUPE-012
HEU-COMP-THERM-021	hct021-13	TUPE-013
HEU-COMP-THERM-021	hct021-14	TUPE-014
HEU-COMP-THERM-021	hct021-44	TUPE-044
HEU-SOL-THERM-001	hst001-1	Rockwell-01
HEU-SOL-THERM-001	hst001-2	Rockwell-02
HEU-SOL-THERM-001	hst001-3	Rockwell-03
HEU-SOL-THERM-001	hst001-4	Rockwell-04
HEU-SOL-THERM-001	hst001-5	Rockwell-05
HEU-SOL-THERM-001	hst001-6	Rockwell-06
HEU-SOL-THERM-001	hst001-7	Rockwell-07
HEU-SOL-THERM-001	hst001-8	Rockwell-08
HEU-SOL-THERM-001	hst001-9	Rockwell-09
HEU-SOL-THERM-001	hst001-10	Rockwell-010
HEU-SOL-THERM-009	hst009-1	ORNL-S1
HEU-SOL-THERM-009	hst009-2	ORNL-S2
HEU-SOL-THERM-009	hst009-3	ORNL-S3
HEU-SOL-THERM-009	hst009-4	ORNL-S4
HEU-SOL-THERM-013	hst0013-1	ORNL-T1
HEU-SOL-THERM-013	hst0013-2	ORNL-T2
HEU-SOL-THERM-013	hst0013-3	ORNL-T3
HEU-SOL-THERM-013	hst0013-4	ORNL-T4
HEU-SOL-THERM-032	hst0032	ORNL-T5
HEU-SOL-THERM-042	hst0042-1	ORNL-C1
HEU-SOL-THERM-042	hst0042-2	ORNL-C2

HEU-SOL-THERM-042	hst0042-3	ORNL-C3
HEU-SOL-THERM-042	hst0042-4	ORNL-C4
HEU-SOL-THERM-042	hst0042-5	ORNL-C5
HEU-SOL-THERM-042	hst0042-6	ORNL-C6
HEU-SOL-THERM-042	hst0042-7	ORNL-C7
HEU-SOL-THERM-042	hst0042-8	ORNL-C8
IEU-COMP-THERM-003	ict003-1	TRIGA_C132
IEU-COMP-THERM-003	ict003-2	TRIGA_C133
LEU-COMP-THERM-008	lct008-01	BW-XI-1
LEU-COMP-THERM-008	lct008-02	BW-XI-2
LEU-COMP-THERM-008	lct008-05	BW-XI-5
LEU-COMP-THERM-008	lct008-07	BW-XI-7
LEU-COMP-THERM-008	lct008-08	BW-XI-8
LEU-COMP-THERM-008	lct008-11	BW-XI-11
LEU-COMP-THERM-009	lct009-26	lct-26
LEU-COMP-THERM-009	lct009-27	lct-27
LEU-COMP-THERM-042	lct042-1	lct042-1
LEU-COMP-THERM-042	lct042-2	lct042-2
LEU-COMP-THERM-043	lct043	IPEN/MB-01
LEU-SOL-THERM-002	lst002-1	ORNL-UO2F2
LEU-SOL-THERM-002	lst002-2	ORNL-UO2F2
LEU-SOL-THERM-007	lst007-14	STACY-14
LEU-SOL-THERM-007	lst007-30	STACY-30
LEU-SOL-THERM-007	lst007-32	STACY-32
LEU-SOL-THERM-007	lst007-36	STACY-36
LEU-SOL-THERM-007	lst007-49	STACY-49
LEU-MET-THERM-015	lmt015	lmt015
U233-COMP-THERM-001	uct001-20	SB-2
U233-COMP-THERM-001	uct001-25	SB-2+h
U233-COMP-THERM-001	uct001-30	SB-3
U233-COMP-THERM-001	uct001-40	SB-4
U233-COMP-THERM-001	uct001-60	SB-6
U233-COMP-THERM-001	uct001-70	SB-7
IEU-COMP-FAST-002	icf002	KBR-18
IEU-COMP-INTER-001	ici001-19	KBR-19
IEU-COMP-INTER-001	ici001-20	KBR-20
IEU-COMP-THERM-005	ict005	KBR-21
HEU-MET-FAST-052	hmf052	FKBN-f2
HEU-MET-FAST-068	hmf068	KBR-22
HEU-MET-FAST-070	hmf070-7	ZPR-9/7
HEU-MET-FAST-070	hmf070-8	ZPR-9/8
HEU-MET-FAST-070	hmf070-9	ZPR-9/9
HEU-MET-INTER-008	hmi008	KBR-23
MIX-COMP-FAST-001	mcf001	ZPR-6/7
MIX-COMP-FAST-005	mcf005	ZPR-9/31
MIX-COMP-FAST-006	mcf006	ZPPR-2
PU-MET-FAST-029	pmf029	pmf029
PU-MET-FAST-032	pmf032	pmf032

Benchmark results are as yet incomplete, but the comparison of results for selected cases can be seen on Fugures 8 to 11.

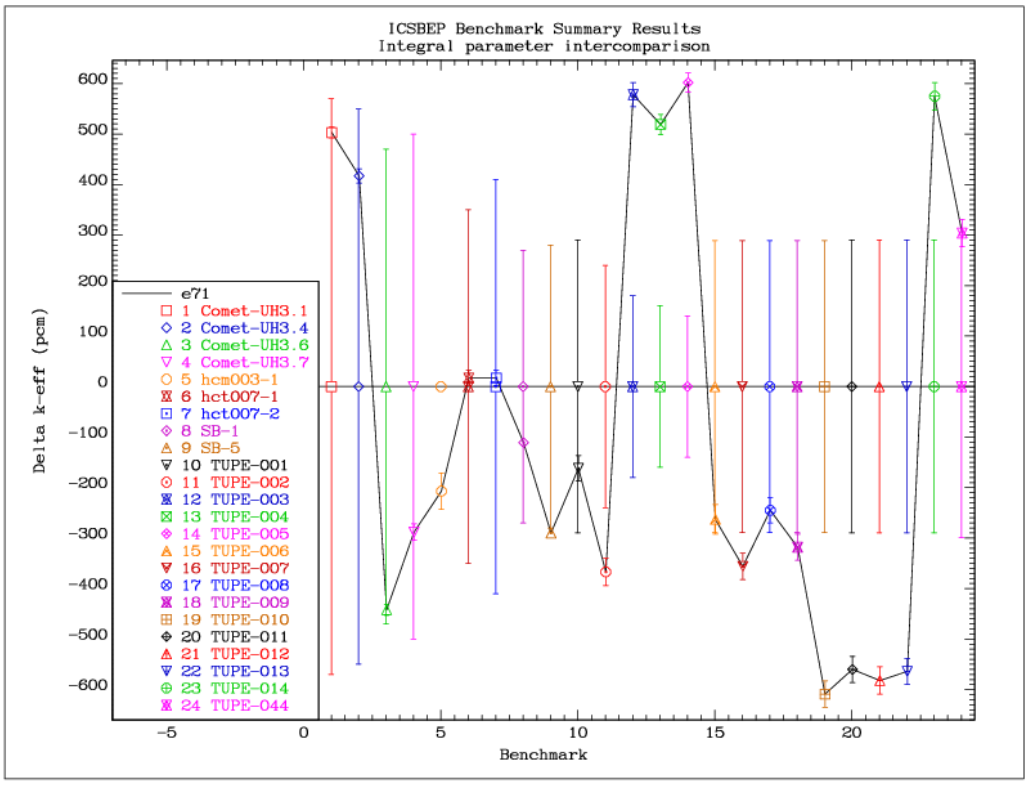

Figure 8: Benchmark results using different evaluated data for ^{16}O.

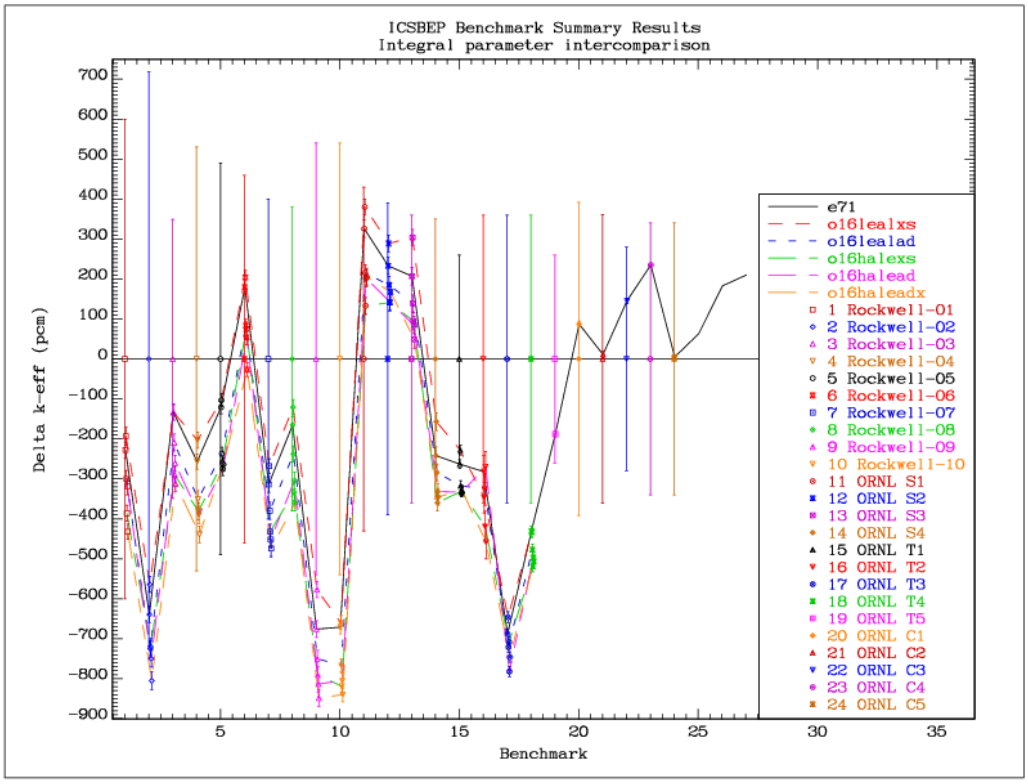

Figure 9: Benchmark results using different evaluated data for ^{16}O.

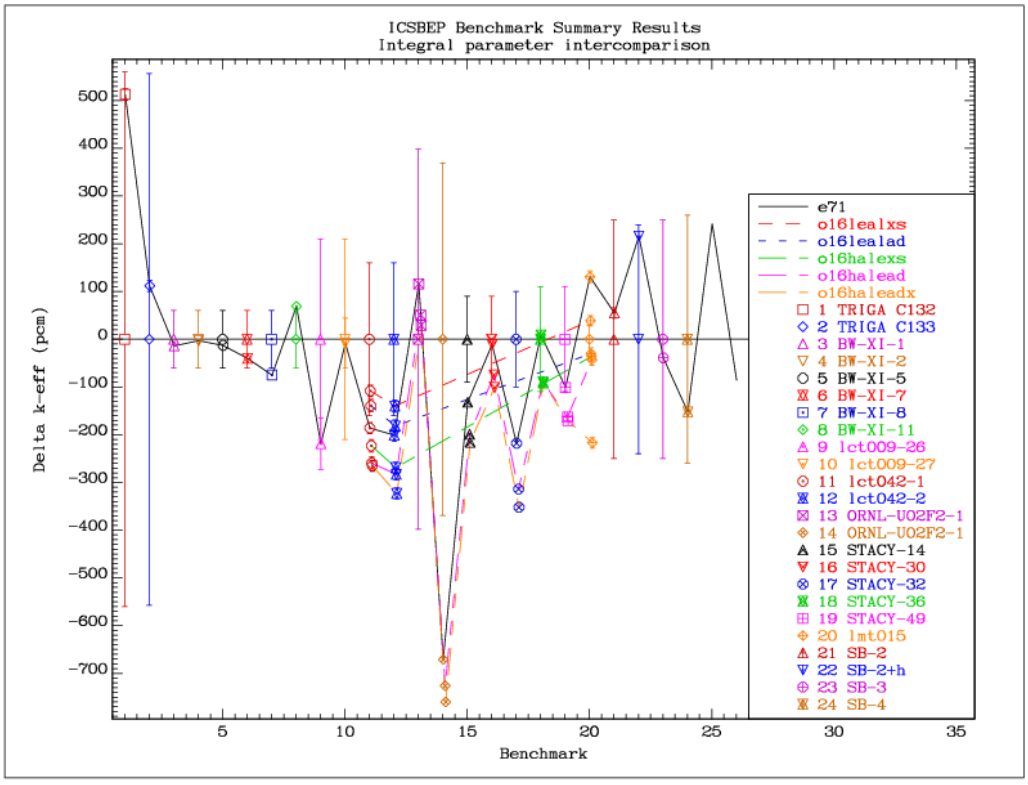

Figure 10: Benchmark results using different evaluated data for ^{16}O.

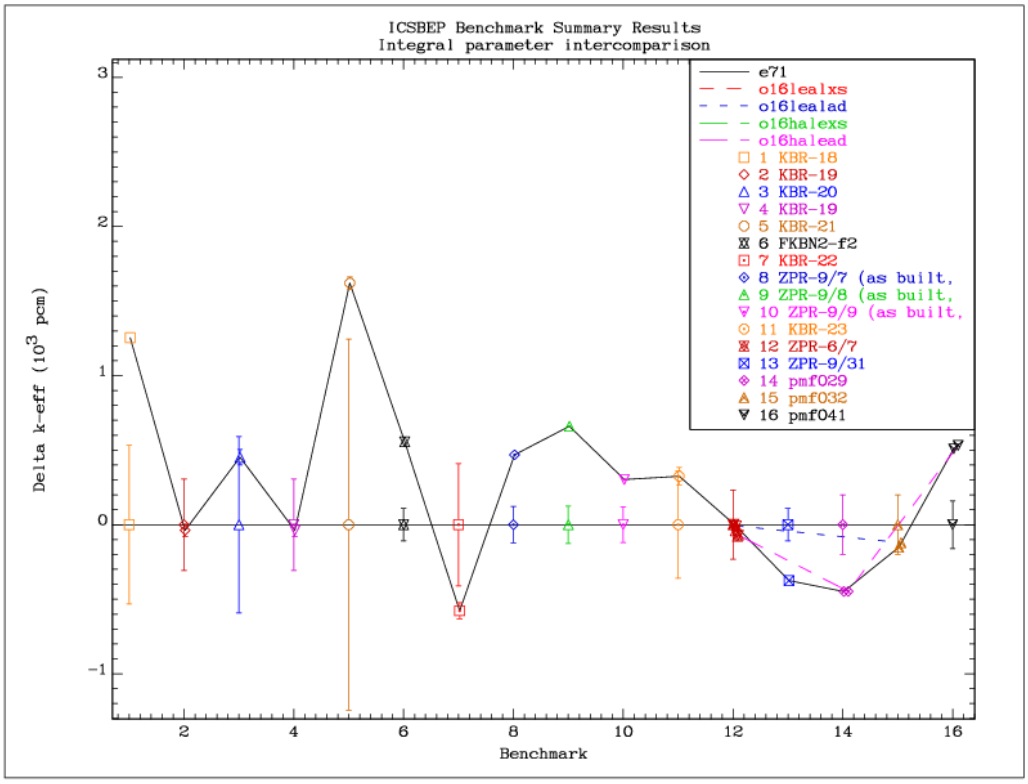

Figure 11: Benchmark results using different evaluated data for ^{16}O.

Conclusions

The Results reflect work in progress within the CIELO Collaboration. No conclusions can be drawn yet.